Research Article | Vol. 27, No. 25 / 9 December 2019 / Optics Express 36708

Optics EXPRESS

Improved efficiency of InGaN/GaN light-emitting diodes with perpendicular magnetic field gradients

JANG-HWAN HAN,[1] JAE-JOON KIM,[2] YOUNG-CHUL LEEM,[1] SANG-JO KIM,[1] WONYOUNG KWAK,[1] WOO-LIM JEONG,[3,4] BEONGKI CHO,[1,2] DONG-SEON LEE,[3,4,5] AND SEONG-JU PARK[1,2,6]

[1]*School of Materials Science and Engineering, Gwangju Institute of Science and Technology, Gwangju 61005, South Korea*
[2]*Department of Nanobio Materials and Electronics, Gwangju Institute of Science and Technology, Gwangju 61005, South Korea*
[3]*School of Electrical Engineering and Computer Science, Gwangju Institute of Science and Technology, Gwangju 61005, South Korea*
[4]*Research Institute for Solar and Sustainable Energies, Gwangju 61005, South Korea*
[5]*dslee66@gist.ac.kr*
[6]*sjpark@gist.ac.kr*

Abstract: The effect of magnetic fields on the optical output power of flip-chip light-emitting diodes (LEDs) with InGaN/GaN multiple quantum wells (MQWs) was investigated. Films and circular disks comprising ferromagnetic cobalt/platinum (Co/Pt) multilayers were deposited on a *p*-ohmic reflector to apply magnetic fields in the direction perpendicular to the MQWs of the LEDs. At an injection current of 20 mA, the ferromagnetic Co/Pt multilayer film increased the optical output power of the LED by 20% compared to an LED without a ferromagnetic Co/Pt multilayer. Furthermore, the optical output power of the LED with circular disks was 40% higher at 20 mA than the output of the LED with a film. The increase of the optical output power of the LEDs featuring ferromagnetic Co/Pt multilayers is attributed to the magnetic field gradient in the MQWs, which increases the carrier path in the MQWs. The time-resolved photoluminescence measurement indicates that the improvement of optical output power is owing to an enhanced radiative recombination rate of the carriers in the MQWs as a result of the magnetic field gradient from the ferromagnetic Co/Pt multilayer.

1. Introduction

High-efficiency GaN-based light-emitting diodes (LEDs) have been extensively developed for use in displays, automobiles, and illumination applications owing to their intrinsic advantages of low energy consumption, high reliability, and environmental benefits [1–3]. Enhancing the internal quantum efficiency (IQE) and light extraction efficiency (LEE) can further increase the efficiency of LEDs. Researchers have recently demonstrated improved IQE by increasing the radiative recombination rate in the multiple quantum wells (MQWs) of the LEDs by introducing high-quality GaN, an electron blocking layer [4], bandgap engineering [5], polarization matching [6], and surface plasmons [7]. The LEE, on the other hand, is controlled by the LED structure, where the flip-chip LED structure emerges as one that simultaneously increases the LEE and the current injection efficiency [8].

Several studies have reported the effect of magnetic fields on the electrical and optical properties of III-V semiconductor devices. In these studies, the carriers were efficiently confined by a uniform external magnetic field at the GaAs/AlGaAs interface [9] and at the MQWs of InGaN/GaN [10] or InGaAs/GaAs [11]. When a strong external magnetic field was applied, the

#371794 https://doi.org/10.1364/OE.27.036708
Journal © 2019 Received 4 Jul 2019; revised 3 Nov 2019; accepted 3 Nov 2019; published 3 Dec 2019

Optics EXPRESS

carrier localization in the potential minima was enhanced owing to the composition fluctuations at the interface and the MQWs. Furthermore, carriers confined in the localized potential minima have a higher carrier recombination rate, resulting in enhanced photoluminescence (PL) intensity [9,10]. It has been reported that the carriers in a Hall-effect sensor can be scattered or trapped under a locally-deposited disk-shaped micromagnet and a magnetic stripe, both of which generate perpendicular magnetic-field gradients [12–16]. In addition to magnetic-field gradients, these micromagnets and magnetic stripes also generate antiparallel magnetic-field directions in the edge and center regions of the magnetic layer that increase the resistance in the Hall-effect sensor via carrier localization and the change in the carrier path from straight to helical.

Recent research has also discussed how a magnetic field influences the performance of inorganic and inorganic LEDs [17–19]. For example, a magnetic field parallel to the InGaN/GaN MQWs can enhance the optical output power in a flip-chip LED with a ferromagnetic CoFe film [17]. To produce this parallel magnetic field, however, a pre-magnetization process with an external magnetic field at high temperature in vacuum is required for the CoFe layer. In this study, we alternately deposited layers of cobalt (Co) and platinum (Pt) to fabricate a 33 nm-thick ferromagnetic cobalt/platinum (Co/Pt) multilayer (FCPM) that spontaneously produced a perpendicular magnetic field without using a high-temperature, pre-magnetization process.

Although the carrier motion in a perpendicular magnetic field is different from that in a lateral field, no reports have yet been made on the effect of a perpendicular magnetic field gradient on the performance of InGaN/GaN MQWs LEDs. As previously reported, when exposed to a lateral magnetic field gradient, the carriers scatter helically as they drift from the strong magnetic field region to the weak magnetic field region [17]. When exposed to a perpendicular magnetic field, however, the carriers are scattered or trapped temporally [14,15].

Herein, we report the enhanced optical output power of InGaN/GaN MQWs in flip-chip LEDs in the presence of a nonuniform perpendicular magnetic field arising from a FCPM continuous film or circular disk array deposited on the *p*-ohmic reflector of the LEDs. In addition, we compare the results of the optical output power in the presence of a lateral magnetic field gradient from our previous report [17] with the results using a perpendicular magnetic field gradient herein. Our results demonstrate that the circular FCPM disks, deposited on the *p*-ohmic LED reflector, generate a stronger magnetic field gradient than the FCPM film across the internal carriers in the MQWs. Therefore, the magnetic field gradients induced by the circular FCPM disks were more effective for enhancing carrier recombination in the LEDs than the magnetic field gradients induced by the FCPM film.

2. Experiment

Alternating layers of Co and Pt were deposited to produce magnetic fields across the FCPM in a direction perpendicular to the MQWs, as shown in Fig. 1(a). These layers were placed on the Ni/Ag/Ni *p*-ohmic reflector of a flip-chip LED using a direct-current (DC) magnetron sputtering process. We using tantalum (Ta) as a capping layer and an adhesive layer.

To confirm the generation of perpendicular magnetic fields across the FCPM, the magnetic properties of an FCPM deposited on a separate Si substrate was measured (inset of Fig. 1(b)) using a vibrating sample magnetometer (VSM; Lake Shore Cryotronics). The FCPM exhibited perpendicular anisotropic magnetic behavior despite the lack of pre-magnetization via an additional high-temperature magnetization process. This was possible because the spin and orbital magnetic moments of the Co and Pt were asymmetrically realigned to the perpendicular direction by the hybridization process, whereupon the orbital hybridization at the Co/Pt layer interface spontaneously produced a magnetic field in the perpendicular direction [20,21].

The magnetic field strength and anisotropy were maximized via optimizing the Co and Pt layer thicknesses and the number of Co/Pt layer pairs. On the one hand, a Co layer that is too thin will allow the Co/Pt interface to be intermixed during the DC sputtering process [22]. On the other

Optics EXPRESS

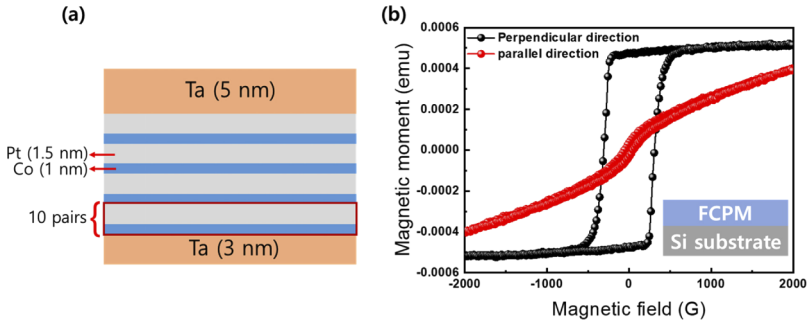

Fig. 1. (a) Schematic of the ferromagnetic Co/Pt multilayer (FCPM) structure and (b) the vibrating sample magnetometer (VSM) characteristics of the ferromagnetic Co/Pt multilayer on a Si substrate. (Inset) Schematic of the FCPM film used for the VSM measurements on a 1 cm × 1 cm Si substrate.

hand, a Co layer thickness greater than 7 to 8 monolayers (~1.3 nm) can cause the magnetic field to tilt from a perpendicular to a lateral direction [22]. Therefore, to maintain the perpendicular magnetic field, we kept the Co layer thickness at 1 nm in this study. It has also been reported that, with increasing number of Co/Pt layer pairs, the magnetic field strength increases while the effective perpendicular anisotropy gradually decreases [23]. Therefore, we deposited 10 pairs of 1 nm-thick Co and 1.5 nm-thick Pt layers as the FCPM on the *p*-ohmic reflector, as shown in Fig. 1(a). The VSM measurement of the FCPM magnetic field in Fig. 1(b) clearly exhibits a square hysteresis loop with a remanent magnetic field of 0.18 T, mostly in the out-of-plane (i.e., perpendicular) direction.

Next, we fabricated flip-chip LEDs with a size of 300 μm × 300 μm, as shown in Figs. 2(a)–2(f). The LED had an emission wavelength of 460 nm and comprised an undoped GaN layer (4 μm), a Si-doped *n*-GaN layer (2 μm), five periods of InGaN/GaN (3 nm/7 nm) MQWs, and a Mg-doped *p*-GaN layer (200 nm). The *p*-GaN layer was partially etched with inductively coupled plasma to expose the *n*-GaN layer. After deposition of the Ni/Ag/Ni (5 nm/120 nm/2 nm) layers as a *p*-ohmic reflector via electron-beam evaporation, the LED was annealed at 400 °C for 1 min in air to achieve a good ohmic contact to the *p*-GaN layer. Subsequently, Cr/Au layers as *n*- and *p*-electrodes were deposited using electron-beam evaporation. The *p*-electrode was isolated from the FCPM to prevent the injection of spin-polarized carriers into the InGaN/GaN MQWs, as shown in Figs. 2(d) and 2(e). We note that, when the electrical current was injected through the magnetic layer, the emitted light was circularly polarized owing to the carrier recombination between the spin-polarized electrons and the heavy holes [24,25]. Finally, 10 pairs of Co/Pt (1 nm/1.5 nm) multilayers were deposited on the Ta (3 nm)/Ni/Ag/Ni *p*-ohmic reflector to supply the magnetic field to the LEDs in the perpendicular direction, where the Ta layer functioned to improve the adhesion between the *p*-ohmic reflector and the FCPM. Another 5 nm-thick Ta layer was then deposited as a capping layer to prevent oxidation of the top Co layer in the FCPM, as shown in Figs. 2(d), 2(e), and 1(a). In addition to the FCPM film and for comparative purposes, an array of circular FCPM disks with a 10 μm diameter and a 5 μm spacing were fabricated using a photolithography process, as shown in Fig. 2(d)–2(f).

The electrical and optical properties of the LEDs were measured using a parameter analyzer (HP-4155A) and a calibrated Si photodiode connected to an optical power meter. Time-resolved photoluminescence (TR-PL) spectra were measured at 10 K using a wavelength-tunable mode-locked Ti:sapphire laser with a pulse width of 150 fs and repetition frequency of 80 MHz within a time scale of 200 ns. In the excitation process, the laser beam penetrated the LED from the bottom side of the sapphire substrate and excited the MQWs in the LED.

Optics EXPRESS

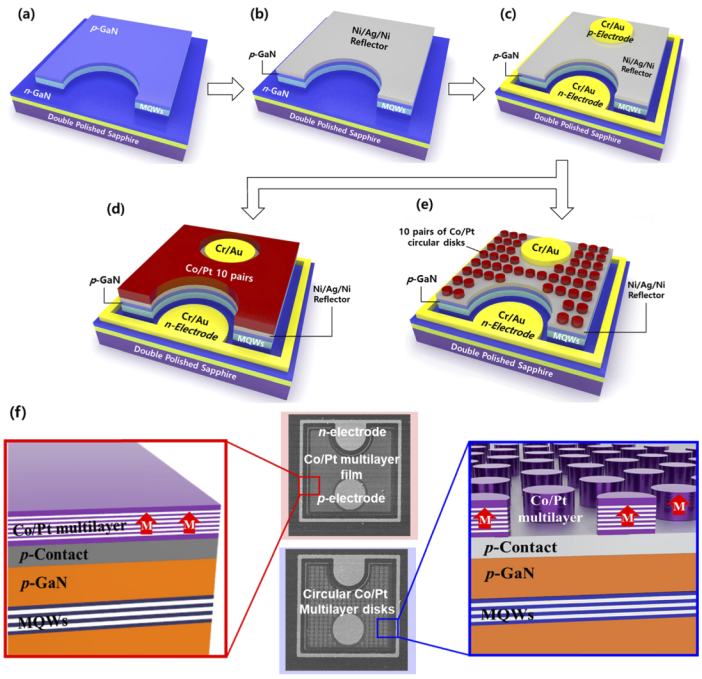

Fig. 2. Schematic of the fabrication steps for flip-chip LEDs with a Co/Pt multilayer: (a) mesa etching to expose the *n*-contact area, (b) deposition of the *p*-ohmic reflector on the *p*-GaN, (c) deposition of the *n*- and *p*-electrodes on the *n*-GaN and *p*-ohmic reflector, (d) deposition of the Co/Pt multilayer film, and (e) circular FCPM disks on the *p*-ohmic layer. (f) SEM images (center) and schematics of the LEDs with a Co/Pt film (left) and with disks (right).

3. Results and discussion

The current–voltage (I-V) characteristics were obtained for the LEDs without an FCPM, with a FCPM film, and with circular FCPM disks, and are shown in Fig. 3(a). The forward voltages of the three different LEDs were all 3.5 V at 20 mA, but the series resistances of the LEDs containing an FCPM film (12.4 Ω) and circular FCPM disks (13.8 Ω) were slightly increased from that of the reference LED (11.8 Ω), as shown in the inset of Fig. 3(a). This increased series resistance in the LEDs with the FCPM is attributed to increased carrier scattering and the change in carrier trajectory from straight to helical owing to the nonuniform magnetic field, as reported in the previous studies [9,14,15]. This mechanism is illustrated in the simple schematic diagrams in Figs. 4(a) and 4(b). The perpendicular magnetic fields generated by the FCPM film and circular disks are strong at the edge region (i.e., outer core) and relatively weak at the center region (i.e., inner core) [13,14], which produces the magnetic field gradient. Further, the magnetic field direction is upward in the inner core and downward in the outer core of the FCPM (Fig. 4(a)). Therefore, the motion of the carrier varies depending on its kinetic energy, as denoted by the paths marked 1 to 3 in Fig. 4(b). [12,13,26]. Carriers with low or high kinetic energies are scattered in various directions and exhibit a helical motion while scattered backward (1 in Fig. 4(b)) or penetrate edge to edge (3 in Fig. 4(b)). However, carriers that possess the appropriate kinetic energy (i.e., resonant energy) move along the interface between the outer and inner core with a snake-like motion. (2 in Fig. 4(b)) [13–15]. Therefore, the series resistance of the LED with an FCPM (Fig. 3(a)) is slightly increased owing to carrier scattering or temporal trapping under the nonuniform perpendicular magnetic field [13,14,26].

Optics EXPRESS

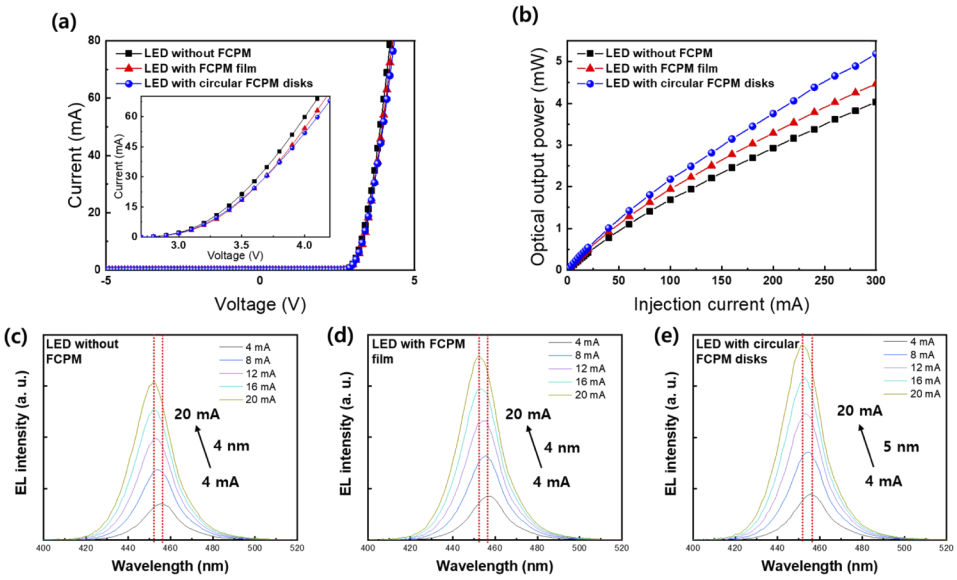

Fig. 3. (a) Current–voltage (I-V) characteristics, (Inset: detail of the I-V curve) (b) optical output power of an LED without a ferromagnetic Co/Pt multilayer (FCPM) (black squares), with an FCPM film (red triangles), and with circular FCPM disks (blue circles). (c–e) Electroluminescence spectra at injection currents between 4 mA and 20 mA of an LED (c) without an FCPM, (d) with an FCPM film, and (e) with circular FCPM disks.

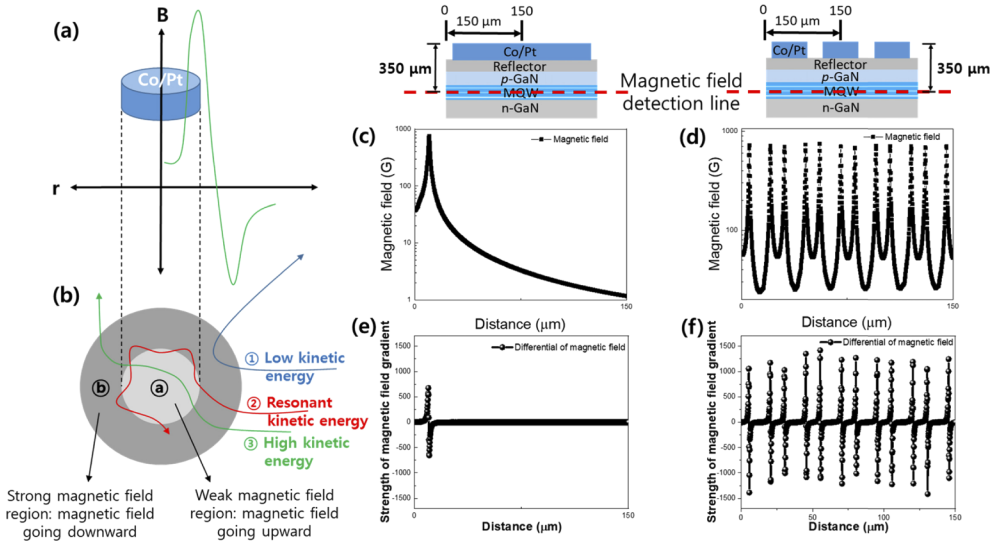

Fig. 4. Schematics of (a) the magnetic field profile in the circular disk of a ferromagnetic Co/Pt multilayer and (b) the carrier trajectory induced by the local magnetic fields and kinetic energy of the carriers. The region marked "a" possesses an upward magnetic field direction where the field strength is relatively weak and the region marked "b" possesses a downward magnetic field direction where the field strength is relatively strong. Carrier trajectories with low (marked as 1), resonant (marked as 2), and high kinetic energy (marked as 3) react differently to the perpendicular magnetic field gradient. Finite Element Method Magnetics simulations of the magnetic field profiles of the (c) ferromagnetic Co/Pt multilayer film and (d) circular ferromagnetic Co/Pt multilayer disks. The strength of the magnetic field gradient of the (e) film and (f) circular disks.

Optics EXPRESS

Figure 3(b) shows the optical output power of an LED without an FCPM, that with an FCPM film, and that with circular FCPM disks. The optical output power of the LED with an FCPM film is increased by 20% at 20 mA compared with that of the LED without an FCPM. Furthermore, the optical output power of an LED with circular FCPM disks is 40% higher than the output of the LED with an FCPM film. This significant optical output power increase of the LEDs with a FCPM film and with circular FCPM disks is attributed to the altered carrier trajectory and carrier localization in the In-rich regions, which are induced by the magnetic field gradients. More carriers are shifted laterally and propelled towards the In-rich regions by the perpendicular magnetic field gradient, where the strong localization leads to efficient recombination. Consequently, the enhanced carrier localization increases the radiative recombination rate in the MQWs of the LED with an FCPM.

Figures 3(c) to 3(e) show the electroluminescence spectra of LEDs with and without FCPMs, which support the conclusion that the optical output power enhancement originates from a higher rate of radiative recombination. As the current was increased from 4 to 20 mA, the peak positions shifted by 4 nm in the LEDs with and without an FCPM film and by 5 nm in the LED with circular FCPM disks. This occurred even though the optical output powers are higher in LEDs with an FCPM. Further, the peak shift was 4 nm for all three LEDs when the current was adjusted to produce the same optical output power in the three LEDs. Previous research indicates that, because the optical output power increases without changing the photoluminescence and electroluminescence peak position or creating a significant blue shift, the enhanced optical output power is mainly owing to increased radiative recombination and decreased nonradiative recombination via increased carrier localization [9,11].

Even though the 20% increase in optical output power of the LED with the FCPM film is similar to the output of an LED with a ferromagnetic CoFe film in a previous study [17], the 0.18 T magnetic field in our study is half the magnetic field strength in the previous study. The increase in optical output power caused by carrier recombination under magnetic fields is generally proportional to the increase of the magnetic field strength [9,11], and thus our results indicate that perpendicular magnetic field gradients are more effective at localizing or diffusing carriers in LEDs than lateral magnetic field gradients. This improved radiative recombination is the result of carriers being scattered in more varied directions when exposed to a perpendicular magnetic field gradient than a lateral magnetic field gradient [12,14,17], which increases the probability of these scattered carriers becoming trapped in the In-rich regions for a wider area of MQWs [14].

Comparing the optical output power of an LED with a continuous FCPM film to that with circular FCPM disk array (Figs. 3(a) and 3(b)), the LED with circular FCPM disks demonstrated the highest series resistance and optical output power, indicating that the circular FCPM disks can improve LED efficiency more than an FCPM film. To investigate this in more detail, we simulated the magnetic field profiles and magnetic field gradient intensities for the two different FCPM structures using the Finite Element Method Magnetics software. Figures 4(c) and 4(d) show the simulated magnetic field profiles and Figs. 4(e) and 4(f) show the magnetic field gradient intensities. The results represent the magnetic field gradient intensity 350 μm from the FCPM where the MQWs exist. Figures 4(d) and 4(f) show that the LED with circular FCPM disks has a higher intensity and steeper magnetic field gradient than the LED with an FCPM film.

Although the intensity of the magnetic field gradient was much higher in the circular FCPM disks than in the FCPM film, the optical output power only increased by 40%. While we initially expected that the improved magnetic field gradient from the circular FCPM disks would enhance the efficiency of LEDs owing to the wider area of influence upon the carriers, the optical output power increase was not comparable to the magnetic field gradient increase. This result is attributed to the magnetic field overlap in the regions between the circular FCPM disks, as shown in Fig. 4(d). The wider and stronger magnetic field existing between the circular FCPM

Optics EXPRESS

disks restrict the carrier movement in the lateral direction [13,14], and thus the carriers cannot be localized sufficiently in the In-rich region between the circular FCPM disks. We therefore expect that a larger efficiency increase is feasible by optimizing the shape, size, and spacing of the magnetic field.

To further investigate the influence of the magnetic field gradient on the carrier recombination process in the MQWs, TR-PL measurements were performed on the three LEDs, as shown in Fig. 5. Because the TR-PL decay time is related to the carrier localization and recombination efficiency, a decrease in decay time indicates that more carriers are strongly localized in the MQWs and thus efficiently recombined [27,28]. The decay times τ_1 and τ_2 were obtained by fitting the data to the double exponential function, $I(t) = A_1 e^{(-t/\tau_1)} + A_2 e^{(-t/\tau_2)}$, where A_1 and A_2 are normalization constants and t is time constants. The fast decay times were observed to be 3.06, 2.57, and 2.23 ns for the LEDs without an FCPM, with an FCPM film, and with circular FCPM disks, respectively. The fast decay time is related to the carrier's movement from weak localized states (i.e., shallow localized state) to strong localized states (i.e., deep localized state), radiative recombination, and nonradiative recombination [27–29]. Weak and strong localized states are created during the growth of InGaN/GaN MQWs, both of which act as radiative recombination centers [29,30]. In general, carriers easily escape from weak localized states, but they can strongly be localized even in weak localized states when the magnetic field applied. Additionally, carriers with high energy (i.e., free carrier) and carriers escaped from weak localized states are directed to strong localized states such as In-rich regions by the magnetic field and magnetic field gradient. Consequently, the radiative recombination is increased by the magnetic field, which helps to reduce the fast decay time [29,30]. Therefore, a decreased fast decay time indicates that the LEDs with magnetic fields quickly confine more carriers from the weak localized states to the strong localized states, thereby increasing the radiative recombination rate [27,29]. As time goes on, carriers with high energy would be recaptured into strong localized states during slow decay time [29]. The slow decay times of these three LEDs were observed to be 24.84, 22.59, and 18.26 ns, respectively. The decrease in the slow decay time occurs due to more carriers with high energy are rapidly and strongly captured by the magnetic field into the strong localized state. The overall decrease in the TR-PL decay time is owing to the increased carrier density via the band-filling effect at the localized state. This results in an increased radiative recombination rate because of the enhancement of the Coulomb screening via the internal electric field owing to the fully occupied localized state [17,31].

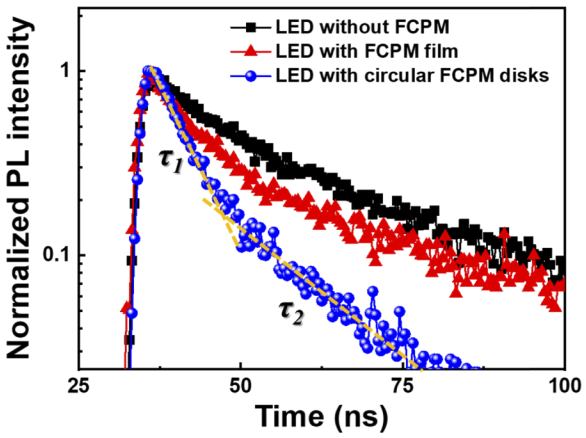

Fig. 5. Time-resolved photoluminescence spectra of LEDs without an FCPM (black squares), with an FCPM film (red triangles), and with circular FCPM disks (blue circles).

Optics EXPRESS

Therefore, based on the TR-PL data, the effect of the magnetic field and the magnetic field gradient on the recombination process of InGaN/GaN MQWs LEDs can be summarized such that the carriers are more strongly localized to the potential minima and these localized carriers produce a faster radiative recombination, which results in enhanced optical output power. Also, the TR-PL data of LEDs with an FCPM film and circular disks show that a stronger and steeper magnetic field gradient can localize more carriers and more efficiently recombine the carriers radiatively. The decay time was shortest in the LED with circular FCPM disks, which indicates that this configuration produced steeper magnetic field gradients than present in the LED with an FCPM film. As a result, the carrier lifetime decreased, the radiative recombination rate increased, and the optical output power increased in the InGaN/GaN MQWs LED with circular FCPM disks.

4. Conclusion

In summary, we reported enhanced performance of flip-chip LEDs with InGaN/GaN MQWs including either an FCPM film or circular FCPM disks, where the latter was deposited on the *p*-ohmic reflector layer of the LEDs. The FCPM film enhanced the LED optical output power by 20% at a forward current of 20 mA compared with an LED without an FCPM. Furthermore, at the same forward current, the LED with circular FCPM disks exhibited a 40% higher optical output power than the LED with an FCPM film. This increased optical output power is attributed to the perpendicular magnetic field gradients, which increase the carrier path lengths in the MQWs by creating carrier drift and improved carrier confinement in the potential minima of the InGaN/GaN MQWs. The larger optical output power increase of the LED with circular FCPM disks than that with an FCPM film is owing to the stronger and steeper magnetic field gradients produced by the multiple circular disks. The measurements of the TR-PL decay times of the LEDs with FCPMs indicate that the enhancement in the optical output power of the LEDs can also be attributed to an improved radiative recombination rate in the MQWs. We expect that our approach for improving the optical output power of LEDs by producing perpendicular magnetic fields using an FCPM will provide an alternative route for designing high-efficiency LEDs with different emission wavelengths by combining LEDs with the proper ferromagnetic materials.

Funding

National Research Foundation of Korea (NRF-2017R1A2B2008538); Gwangju Institute of Science and Technology Research Institute (G11950).

References

1. J. Cho, J. H. Park, J. K. Kim, and E. F. Schubert, "White light-emitting diodes: History, progress, and future," Laser Photonics Rev. **11**(2), 1600147 (2017).
2. P. Pust, P. J. Schmidt, and W. Schnick, "A revolution in lighting," Nat. Mater. **14**(5), 454–458 (2015).
3. J. Bhardwaj, J. M. Cesaratto, I. H. Wildeson, H. Choy, A. Tandon, W. A. Soer, P. J. Schmidt, B. Spinger, P. Deb, O. B. Shchekin, and W. Gotz, "Progress in high-luminance LED technology for solid-state lighting," Phys. Status Solidi A **214**(8), 1600826 (2017).
4. Y. K. Kuo, J. Y. Chang, and M. C. Tsai, "Enhancement in hole-injection efficiency of blue InGaN light-emitting diodes from reduced polarization by some specific designs for the electron blocking layer," Opt. Lett. **35**(19), 3285–3287 (2010).
5. S. H. Han, C. Y. Cho, S. J. Lee, T. Y. Park, T. H. Kim, S. H. Park, S. W. Kang, J. W. Kim, Y. C. Kim, and S. J. Park, "Effect of Mg doping in the barrier of InGaN/GaN multiple quantum well on optical power of light-emitting diodes," Appl. Phys. Lett. **96**(5), 051113 (2010).
6. S. P. Chang, T. C. Lu, L. F. Zhuo, C. Y. Jang, D. W. Lin, H. C. Yang, H. C. Kuo, and S. C. Wang, "Low droop nonpolar GaN/InGaN light emitting diode grown on m-Plane GaN substrate," J. Electrochem. Soc. **157**(5), H501–H503 (2010).
7. M. K. Kwon, J. Y. Kim, B. H. Kim, I. K. Park, C. Y. Cho, C. C. Byeon, and S. J. Park, "Surface-plasmon-enhanced light-emitting diodes," Adv. Mater. **20**(7), 1253–1257 (2008).
8. M. R. Krames, O. B. Shchekin, R. M. Mach, G. O. Mueller, L. Zhou, G. Harbers, and M. G. Craford, "Status and Future of High-Power Light-Emitting Diodes for Solid-State Lighting," J. Disp. Technol. **3**(2), 160–175 (2007).

Optics EXPRESS

9. Q. X. Zhao, B. Monemar, P. O. Holtz, T. Lundström, M. Sundaram, J. L. Merz, and A. C. Gossard, "Magnetic-field-induced localization effects on radiative recombination in GaAs/$Al_xGa_{1-x}As$ heterostructures," Phys. Rev. B **50**(11), 7514–7517 (1994).
10. B. Arnaudov, T. Paskova, O. Valassiades, P. P. Paskov, S. Evtimova, B. Monomer, and M. Heuken, "Magnetic-field-induced localization of electrons in InGaN/GaN multiple quantum wells," Appl. Phys. Lett. **83**(13), 2590–2592 (2003).
11. F. Y. Tsai, C. P. Lee, O. Voskoboynikov, H. H. Cheng, J. Shen, and Y. Oka, "Time-resolved photoluminescence study of InGaAs/GaAs quantum wells on (111)B GaAs substrates under magnetic fields," J. Appl. Phys. **89**(12), 7875–7878 (2001).
12. J. Reijniers, F. M. Peeters, and A. Matulis, "The Hall resistivity of a two-dimensional electron gas in the presence of magnetic clusters with perpendicular magnetization," Phys. E **6**(1-4), 759–762 (2000).
13. J. Reijniers, F. M. Peeters, and A. Matulis, "Electron scattering on circular symmetric magnetic profiles in a two-dimensional electron gas," Phys. Rev. B **64**(24), 245314 (2001).
14. K. S. Novoselov, A. K. Geim, S. V. Dubonos, Y. G. Cornelissens, F. M. Peeters, and J. C. Maan, "Scattering of ballistic electrons at a mesoscopic spot of strong magnetic field," Phys. Rev. B **65**(23), 233312 (2002).
15. A. Nogaret, S. J. Bending, and M. Henini, "Resistance resonance effects through magnetic edge states," Phys. Rev. Lett. **84**(10), 2231–2234 (2000).
16. A. Nogaret, S. Carlton, B. L. Gallagher, P. C. Main, M. Henini, R. Wirtz, R. Newbury, M. A. Howson, and S. P. Beaumont, "Observation of giant magnetoresistance due to open orbits in hybrid semiconductor/ferromagnet devices," Phys. Rev. B **55**(24), R16037 (1997).
17. J. J. Kim, Y. C. Leem, J. W. Kang, J. Kwon, B. Cho, S. Y. Yim, J. H. Baek, and S. J. Park, "Enhancement of the optical output power of InGaN/GaN multiple quantum well light-emitting diodes by a CoFe ferromagnetic layer," ACS Photonics **2**(11), 1519–1523 (2015).
18. J. Kalinowski, M. Cocchi, D. Virgili, P. D. Marco, and V. Fattori, "Magnetic field effects on emission and current in Alq_3-based electroluminescent diodes," Chem. Phys. Lett. **380**(5-6), 710–715 (2003).
19. B. Hu, L. Yan, and M. Shao, "Magnetic-field effects in organic semiconducting materials and devices," Adv. Mater. **21**(14-15), 1500–1516 (2009).
20. N. Nakajima, T. Koide, T. Shidara, H. Miyauchi, H. Fukutani, A. Fujimori, K. Iio, T. Katayama, M. Nývlt, and Y. Suzuki, "Perpendicular magnetic anisotropy caused by interfacial hybridization via enhanced orbital moment in Co/Pt multilayers: Magnetic circular X-ray dichroism study," Phys. Rev. Lett. **81**(23), 5229–5232 (1998).
21. S. Bandiera, R. C. Sousa, B. Rodmacq, and B. Dieny, "Asymmetric interfacial perpendicular magnetic anisotropy in Pt/Co/Pt trilayers," IEEE Magn. Lett. **2**, 3000504 (2011).
22. J. Thiele, C. Boeglin, K. Hricovini, and F. Chevrier, "Magnetic circular X-ray-dichroism study of Co/Pt(111)," Phys. Rev. B **53**(18), R11934(1996).
23. A. Barman, S. Wang, and H. Schmidt, "Ultrafast magnetization dynamics in high perpendicular anisotropy $[Co/Pt]_n$ multilayers," J. Appl. Phys. **101**(9), 09D102 (2007).
24. R. Fiederling, M. Keim, G. Reuscher, W. Ossau, G. Schmidt, A. Waag, and L. W. Molenkamp, "Injection and detection of a spin-polarized current in a light-emitting diode," Nature **402**(6763), 787–790 (1999).
25. E. D. Fraser, S. Hegde, L. Schweidenback, A. H. Russ, A. Petrou, H. Luo, and G. Kioseoglou, "Efficient electron spin injection in MnAs-based spin-light-emitting-diodes up to room temperature," Phys. Rev. Lett. **97**(4), 041103 (2010).
26. D. Uzur, A. Nogaret, H. E. Beere, D. A. Ritchie, C. H. Marrows, and B. J. Hickey, "Probing the annular electronic shell structure of a magnetic corral," Phys. Rev. B **69**(24), 241301 (2004).
27. S. W. Feng, Y. C. Cheng, Y. Y. Chung, C. C. Yang, Y. S. Lin, C. Hsu, K. J. Ma, and J. I. Chyi, "Impact of localized states on the recombination dynamics in InGaN/GaN quantum well structures," J. Appl. Phys. **92**(8), 4441–4448 (2002).
28. Y. Narukawa, Y. Kawakami, S. Fujita, and S. Fujita, "Recombination dynamics of localized excitons in $In_{0.20}Ga_{0.80}N$-$In_{0.05}Ga_{0.95}N$ multiple quantum wells," Phys. Rev. B **55**(4), R1938–R1941 (1997).
29. G. E. Weng, W. R. Zhao, S. Q. Chen, H. Akiyama, Z. C. Li, J. P. Liu, and B. P. Zhang, "Strong localization effect and carrier relaxation dynamics in self-assembled InGaN quantum dots emitting in the green," Nanoscale Res. Lett. **10**(1), 31 (2015).
30. T. Lin, H. C. Kuo, X. D. Jiang, and Z. C. Feng, "Recombination Pathways in Green InGaN/GaN Multiple Quantum Wells," Nanoscale Res. Lett. **12**(1), 137 (2017).
31. Y. J. Lee, C. H. Chiu, C. C. Ke, P. C. Lin, T. C. Lu, H. C. Kuo, and S. C. Wang, "Study of the excitation power dependent internal quantum efficiency in InGaN/GaN LEDs grown on patterned sapphire substrate," IEEE J. Sel. Top. Quantum Electron. **15**(4), 1137–1143 (2009).